A Comprehensive Analysis of Low-Power Operation for Beacon-Enabled IEEE 802.15.4 Wireless Networks

Yu-Kai Huang, *Student Member, IEEE,* Ai-Chun Pang, *Senior Member, IEEE,* and Hui-Nien Hung

***Abstract*—ZigBee, a unique communication standard designed for low-rate wireless personal area networks, has extremely low complexity, cost, and power consumption for wireless connectivity of inexpensive, portable, and moving devices. ZigBee uses the IEEE 802.15.4 standard as its communication protocol for medium access control (MAC) layer and physical (PHY) layer. The IEEE 802.15.4 MAC layer achieves duty-cycle operations by setting two system parameters, $macBeaconOrder$ (BO) and $macSuperFrameOrder$ (SO), to achieve low power consumption for ZigBee devices. This study comprehensively analyzes IEEE 802.15.4 duty-cycle operation. Specifically, a novel analytical model that accommodates a general traffic distribution is developed. An NS-2 based simulation model, which is validated by the developed analytical model is also proposed. Through the experiments conducted by the analytical and simulation models, some important performance-evaluation insights are gained that can be used as guidelines for future low-power ZigBee network deployment.**

***Index Terms*—IEEE 802.15.4, ZigBee, low-power operation, performance analysis.**

I. Introduction

With the success of wireless local area networks, the wireless networking community has been looking for new avenues to enable wireless connectivity to be extended to existing and new applications [13]. The emergence of short-transmission-range wireless devices has furthered the development of wireless personal area networks (WPANs). A WPAN is a wireless network for device inter-connectivity based on individual workspaces. Among the well-known WPAN specifications, ultra-wideband (i.e., IEEE 802.15.3) is designed for high-transmission-rate WPANs [1]. Bluetooth (i.e., IEEE 802.15.1) supports various applications, such as wireless headsets of home audio and computer peripherals, and provides quality of service (QoS) transmissions, particularly for audio traffic [28].

For low-cost wireless devices, ZigBee has emerged as an effective alternative for WPANs. Applications supported by ZigBee includes home automation, remote control and monitoring, and health care [34]. In ZigBee, IEEE 802.15.4 is utilized as the communication protocol for the medium access control (MAC) layer and physical (PHY) layer [2], and supports low data-rate (i.e., 20kbps, 40kbps, and 250kbps). Such low transmission rate and low-cost characteristics make ZigBee suitable for wireless systems comprising unsupervised groups of devices in houses, factories and offices. To facilitate ZigBee network deployment, most devices are unplugged, and rather operated by batteries. Additionally, the target environments in which devices operate can be so complex that changing device batteries becomes difficult or even impossible. Thus, how to achieve efficient energy consumption for devices with small power supplies is critical to ZigBee applications.

IEEE 802.15.4 MAC layer provides a duty-cycle operation by setting two system parameters, $macBeaconOrder$ (BO) and $macSuperFrameOrder$ (SO), such that low power consumption is achieved for ZigBee networks [2]. In addition to determining the duty cycle, the BO and SO parameters collaboratively provide various low-power attributes under a single duty cycle for diverse environments [24]. Simultaneously increasing BO and SO increases the transmission latency and decreases system throughput due to intensive channel contention, whereas simultaneously decreasing BO and SO reduces available bandwidth and increases the energy consumption during beacon reception. Each low-power attribute via setting the BO and SO values has its own impact on transmission and energy efficiency of IEEE 802.15.4 MAC layer. With a very limited bandwidth and power capacity for IEEE 802.15.4 devices, any unnecessary transmission overhead or excessive power consumption resulting from improper BO and SO settings could markedly degrade device performance. Additionally, inappropriate BO and SO settings for a low duty-cycle system may lead to more power consumption than that of a high duty-cycle system with optimal BO and SO values. Unfortunately, IEEE 802.15.4 does not explicitly suggest BO and SO values. To our best knowledge, the settings for BO and SO are based on manual tuning methodologies, which is a time-consuming deployment process. Thus, a comprehensive investigation of low-power operation in IEEE 802.15.4 is necessary.

In the past years, some notable research results have been presented for the analyzing of power saving mode (PSM) in IEEE 802.11 [32], [3], [27]. However, the IEEE 802.11 PSM is very different from IEEE 802.15.4 low-power operation. In the IEEE 802.11 PSM, as the access point is always awake,

Manuscript received November 7, 2008; revised April 25, 2009; accepted July 11, 2009. The associate editor coordinating the review of this paper and approving it for publication was T. Hou.

Y.-K. Huang and A.-C. Pang are with the Graduate Institute of Networking and Multimedia, Department of Computer Science and Information Engineering, National Taiwan University, Taipei 10617, Taiwan, R.O.C. (e-mail: {d94944009, acpang}@csie.ntu.edu.tw).

H.-N. Hung is with the Institute of Statistics, National Chiao Tung University, Hsinchu 30010, Taiwan, R.O.C. (e-mail: hhung@stat.nctu.edu.tw).

Digital Object Identifier 10.1109/TWC.2009.081485

stations can transmit their uplink packets whenever they want to send. Conversely, in IEEE 802.15.4, the coordinator and devices can only communicate during active periods, and enter the sleep phase during inactive periods. The uplink packets generated in an inactive period are buffered, and excessive uplink packet transmissions are generated at the start of the next active period. This situation seldom occurs in the IEEE 802.11 PSM. Therefore, existing analytical models for IEEE 802.11 PSM cannot be applied directly to the low-power operation of IEEE 802.15.4.

Based on the IEEE 802.15.4 specification, Djukic *et al*. [10] proposed a new transport layer protocol for directed diffusion in sensor networks; performance of the proposed protocol was evaluated using NS-2. Mišić *et al*. [19] analyzed the performance of an IEEE 802.15.4-compliant network operating in beacon enabled mode with both downlink and uplink traffic. Lee *et al*. [17] established a realistic environment for preliminary performance evaluation of IEEE 802.15.4 based wireless networks. Lee *et al*. [29] presented a new model for the slotted CSMA/CA (Carrier Sense Multiple Access)/(Collision Avoidance) of IEEE 802.15.4 MAC, and evaluated its throughput limit. Based on a non-stationary Markov chain model, Shu *et al*. [26] provides an analysis that yields the packet loss statistics for the non-acknowledgement mode of an IEEE 802.15.4 system. However, IEEE 802.15.4 power-saving in inactive periods was not addressed in these works. For the inactive period, Sheu *et al*. [24] proposed an adaptive interleaving access scheme that adjusts the superframe structure to control access latency and the bandwidth wastage. Jeon *et al*. [14] proposed a duty-cycle adaptation algorithm for IEEE 802.15.4 which modifies the MAC layer header to monitor MAC status. However, the modification of IEEE 802.15.4 MAC specification in [24], [14] makes the Zigbee implementation less practical as many new IEEE 802.15.4 based devices are manufactured and purchased.

In analyzing low-power operations in IEEE 802.15.4, Neugebauer *et al*. [20] proposed a new algorithm for BO adaptation in IEEE 802.15.4 star-topology networks, and analyzed the performance using their own developed simulator. Shu *et al.* [25] implemented a C-based simulation model for IEEE 802.15.4 MAC to determine optimal BO and SO values, such that overall network energy consumption was minimized. However, their experimental results [20], [25] were based on ideal assumptions for IEEE 802.15.4 MAC-layer operations. For instance, packet collisions resulting from the MAC-layer CSMA/CA were not considered. In this paper, we develop a complete analytical model and adopt the well-known NS-2 network simulator [31] to realistically model IEEE 802.15.4 MAC behavior.

In the analysis of this work, low-power operation in IEEE 802.15.4 is investigated comprehensively. Performance metrics, including queuing drop rate, goodput, and power consumption, are evaluated using the analytical and simulation models. The proposed analytical model can accommodate a general traffic distribution to capture the diverse traffic characteristics in various applications. The NS-2 based simulation validated by analytical results is also developed. Although the IEEE 802.15.4 module has been provided in NS-2, the lack of full support for low-power operation makes our experiments especially for energy consumption difficult to be derived. Additionally, few traffic distributions are provided in the existing NS-2 simulation model. Therefore, we make considerable effort to revise the NS-2 module to supply a complete low-power operation under the traffic load with diverse distributions. The performance evaluation conducted using the proposed analytical model and NS-2 yields many significant insights under various system parameters, including BO, SO, buffer size, and traffic load distribution.

The remainder of this paper is organized as follows: Section II describes the MAC protocol for IEEE 802.15.4. Section III illustrates low-power operations. In Section IV, the proposed analytical model for low-power operation is presented. In Section V, a series of experiments are conducted using the proposed analytical model and NS-2 to investigate the system performance under various wireless environments. Section VI provides conclusions.

II. An Overview of IEEE 802.15.4 MAC

The IEEE 802.15.4 standard defines the PHY and MAC sublayer specifications for low-rate WPANs (LR-WPANs) [2]. This standard supports wireless communications between devices with minimal power consumption, and typically operates in a personal operating space of 10 meter or less. The IEEE 802.15.4 standard defines two medium-access modes: the nonbeacon-enabled mode and beacon-enabled mode. In the nonbeacon-enabled mode, arbitration of medium access is only distributed among wireless devices based on CSMA/CA. In addition to CSMA/CA-based transmissions, the beacon-enabled mode provides a contention-free guaranteed time slot (GTS) mechanism that supports time-critical data delivery. Additionally, low-power operation is provided using a beacon-based superframe structure, which is described below. This work focuses on the IEEE 802.15.4 beacon-enabled mode; the details of the nonbeacon-enabled mode can be found in [2].

In the IEEE 802.15.4 specifications, a superframe is activated by a beacon issued by a PAN coordinator, and has an active and inactive portion. The duration (also called beacon interval (BI)) of a superframe ranges from 15ms to 245s. The coordinator and devices can communicate during active periods and enter the low-power phase during inactive periods. The length of BI, which is determined by the parameter $macBeaconOrder$ (BO), can be derived as

$$BI = 2^{BO} \times aBaseSuperFrameDuration,\ 0 \leq BO \leq 14$$

where $aBaseSuperFrameDuration$ is the minimum duration of a superframe. Furthermore, the parameter SO determines the length of an active period $SuperframeDuation$ (SD); SD is be derived as follows.

$$SD = 2^{SO} \times aBaseSuperFrameDuration,\ 0 \leq SO \leq BO$$

The active portion with 16 time slots has three parts: a beacon, a contention access period (CAP), and a contention free period (CFP). The beacon is transmitted by the coordinator at the start of slot 0, and the CAP follows immediately after. The CAP, uses a slotted CSMA/CA approach for devices accessing the channel and transmitting non-time-critical messages and MAC commands. The CFP, uses the standard protocol of GTS

for devices to exclusively occupy the transmission time slots. The coordinator permits at most seven GTSs for real-time services during the CFP. The GTS allocation information is attached in the beacon frame. Notably, the length of a CAP and CFP in a superframe is determined by the coordinator based on real-time and non-real-time traffic demands.

The slotted CSMA/CA maintaining three counters in each device for channel access control. Notably, NB is the number of backoff trials (i.e., backoff stage) for packet transmission. BE is the backoff exponent for generating a random backoff duration for which a device has to wait before attempting carrier sensing, and CW is the value of the contention window slots for clear channel assessment (CCA) after the random backoff duration. Based on the counters, the medium-access process of slotted CSMA/CA for a device is as follows. First, a device with a packet pending for transmission selects a random backoff counter in the range of [0, $2^{BE}-1$]. The backoff counter value then decreases automatically at every slot. When the backoff counter becomes zero, the device begins carrier sensing (CCA) in the following slots. If either slot is sensed busy, NB and BE are increased by 1, CW is reset to 2, and the backoff count-down process with a new random backoff counter value is executed; otherwise, the device has an opportunity to transmit the packet. A transmission is considered failed when NB achieves K, where K has a default value of 5.

III. IEEE 802.15.4 Low-Power Operation

The IEEE 802.15.4 standard is utilized to support low-rate transmission over WPANs. With low-rate data deliveries, IEEE 802.15.4 devices do not need to be always active in a superframe. To achieve the required low power consumption, the IEEE 802.15.4 standard defines a low-power operation to achieve low duty-cycle operations. The duty cycle in IEEE 802.15.4 is defined as the proportion of time during which a system operates. When the duty cycle $\leq 100\%$, devices can turn off their transceivers during inactive periods to reduce power consumption. The duty cycle is the ratio of the length of an active period SD to the length of a BI, and is calculated as $(\frac{1}{2})^{BO-SO}$.

Based on the derivation of the duty cycle, the duty cycles supported by IEEE 802.15.4 have bases of $1/2$, and $0 \leq (BO-SO) \leq 14$. A large duty cycle results in high power consumption for IEEE 802.15.4 devices. Additionally, a specific duty cycle can be achieved by setting several different (BO, SO) pairs. For example, the (BO, SO) pairs, $(5, 3)$ and $(6, 4)$, have the same duty cycle $1/4$ (i.e., 25%). However, different pairs under the same duty cycle provide various low-power attributes, and have differing impacts on throughput and energy efficiency. To further understand low-power operation of IEEE 802.15.4, the effects of duty cycle and low-power attributes on system performance are elaborated as follows.

- Effect of Duty Cycle.
  In IEEE 802.15.4, a large duty cycle with a long active period provides increased bandwidth resources for devices, such that throughput is increased. Since the system stays in awake mode for a long time, power consumption is increased. Conversely, a system that operates in a relatively lower duty cycle consumes less power. However, transmission latency increases for the packets generated in the extended inactive period. When the duty cycle is extremely small, the throughput could be reduced significantly because of insufficient bandwidth. Therefore, a trade-off exists for duty-cycle setting between system throughput and device energy consumption.
- Effect of Low-Power Attributes.
  Figure 1 presents two examples of a superframe structure for different (BO, SO) settings (i.e., $(C, C-1)$ and $(C-3, C-4)$) of the duty cycle 50%. When a large BO is used, inactive periods are extended such that transmission latency increases. Also, with a long inactive period, the buffered packets will contend the channel intensively at the start of the next active period. Then the throughput is degraded due to increased packet drop rate. Additionally, the intensive channel contentions result in significant carrier-sensing overhead for devices, and thus increases energy consumption.
  Conversely, when BO decreases, the length of the superframe (i.e., BI) decreases and the beacon transmission frequency increases exponentially. As beacon overhead increases, available bandwidth for data delivery decreases. Furthermore, overall power consumption increases due to increases in beacon transmissions. However, a small BO benefits the throughput since the buffered packet transmissions are relieved under a shortened inactive period.

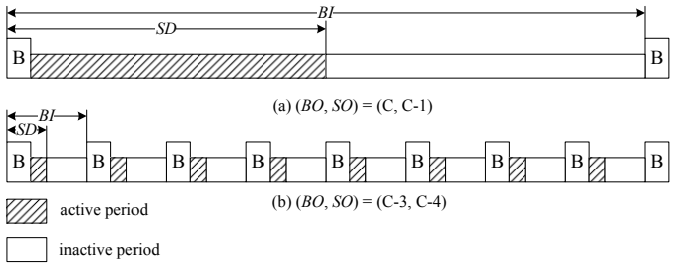

Fig. 1. Different BO and SO values of 50% duty cycle.

In summary, many performance trade-offs exist when setting BO and SO parameters. The system performance affected by duty cycle and low-power attributes is not easily or intuitively predicted. The following sections, we present the analytical model and use numerical results to demonstrate their influence on the system performance, and to provide the insights into low-power operation in IEEE 802.15.4.

IV. Analytical Model for Low-power Operation

In this section, system performance during low-power operation is investigated comprehensively via a mathematical analysis. For a traffic load with a general distribution, this model can determine the system performance including queuing drop rate, goodput, and power consumption.

A. Analytical Model Overview

In this analysis, we assume a star topology with 1 PAN coordinator and N functionally identical devices are assumed. The buffer size of devices is M and the packet arrival rate

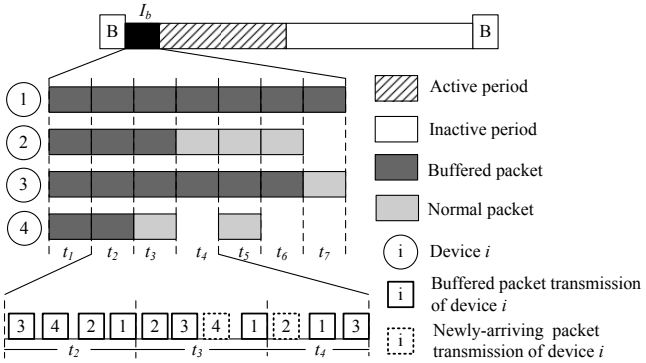

Fig. 2. An example of packet transmission in I_b.

is λ. We assume all MAC frames have the same length [4], which is widely adopted in MAC protocol analysis. The time unit used in the analysis is the backoff slot defined in IEEE 802.15.4. Without loss of generality, the optional function for acknowledging receipt of packets is disable, and a single CCA (i.e. $CW = 1$) is used in the analysis. The complete superframe structure in IEEE 802.15.4, including the active period and inactive period, is examined. Packets arriving from the upper layer during the inactive period are buffered and transmitted at the start of the next active period. To transmit the buffered packets, devices intensively contend the channel at the start of the active period, such that system performance is seriously degraded. Thus the buffered packet transmission in IEEE 802.15.4 is thoroughly investigated.

In the analysis, I_b denotes the interval for transmitting all buffered packets during the inactive period. In the remainder of this work, the "buffered packets" are the packets buffered in the inactive period. Based on long-term [1] fairness of CSMA/CA [6], we assume the $(k+1)$st buffered packet of one device cannot be served until the kth buffered packets of all other devices are transmitted. The interval I_b can then be virtually partitioned into several time regions. The kth buffered packets of all devices are transmitted in each virtual time region t_k $(1 \leq k \leq M)$. As shown in Figure 2, interval t_2 includes the transmission of the second buffered packets of all devices. In addition to serving buffered packets, each virtual time region could handle the arrival of new packet for the devices without buffered packets. In t_3 of Figure 2, Devices 1, 2 and 3 transmit their buffered packets, while Device 4 acts as a normal device to send its new packet.

Based on the structure of the virtual time regions, the proposed analytical model is presented in three parts. Subsection IV-B models the MAC behavior in a virtual time region t_k. Packet drop due to consecutive channel sensing failures, and packet collision due to simultaneous transmissions are considered in this subsection. The fraction of successful transmission time and fraction of transmission/sensing time for a device in a virtual time region are then derived. Subsection IV-C models the distribution of buffered packets by the second-order Edgeworth approximation method. This model accommodates packet inter-arrival times following a general distribution. In Subsection IV-D, packet transmissions in I_b and the remaining active period are considered separately, and system performance measures, including queuing drop rate, goodput and energy consumption, are derived.

[1]Most IEEE 802.15.4 applications are for long-time monitoring and data collection.

TABLE I
NOTATIONS USED IN ANALYTICAL MODEL

Notation	Description
N	The network size
M	The buffer size
K	The maximum number of sensing failures
R_{sv}	The duration for serving a packet
λ	The packet arrival rate
α	The sensing failure probability
τ	The sensing attempt probability
ρ	The transmission probability
$\eta_{tx/ca/sc}$	The fraction of transmission/sensing/successful transmission time for a device
$T_{ca/tx/bn}$	The time spent for CCA/transmission/beacon receiving
$P_k(t)$	The probability that more than k packets arrive in the inactive period t
t_k	The interval for serving the kst buffered packets of all devices
Ψ_k	The state vector for t_k in the system
$\psi_k^{[n]}$	The probability that n saturated devices exist in t_k
$s_k(i,j)$	The transition probability from $\psi_k^{(i)}$ to $\psi_{k+1}^{(j)}$
I_b	The interval for transmitting all packets buffered in the inactive period
$\Upsilon_{sc/tx/rx/sp/id}$	The fraction of total successful transmission/transmission/receiving/sleep/idle time for a device
$E_{tx/rx/sp/id}$	The energy expenditures per time unit for transmitting/receiving/sleep/idle
$\epsilon_{si/it/ir}$	The energy expenditures for the sleep-idle/idle-transmitting/idle-receiving transitions
$T_{si/it/ir}$	The time spent for sleep-idle/idle-transmitting/idle-receiving transitions
$\Phi_{si/it/ir}$	The frequency of sleep-idle/idle-transmitting/idle-receiving transitions
D	The queuing drop rate
G	The Goodput
E	The total energy consumption

B. Modeling IEEE 802.15.4 MAC Behavior

To model the MAC behavior in a virtual time region t_k, the devices transmitting the buffered packets are considered saturated devices, while the remaining devices are considered unsaturated devices with a packet arrival rate λ. The MAC behavior in t_k can be modeled as a heterogenous network with N' saturated devices and $N - N'$ unsaturated devices. The proposed model is modified from the renewal process

concept for homogenous networks [18]. The goal of our model is to derive the fraction of successful transmission time, transmission time, and sensing time of a saturated and unsaturated device.

We assume that the probability of sensing the channel in a randomly chosen time slot is independent from other devices, and independent of the number of retransmission trials for each device. Specifically, this independent assumption is the counterpart to that in [8], [5] for the performance analysis of IEEE 802.11 MAC protocol, and is adopted in the IEEE 802.15.4 study [30]. Since two classes of devices (i.e., saturated and unsaturated devices) are considered, notations $(.)$ is used for unsaturated devices, and $(.)^{'}$ is used for saturated devices. Additionally, $\overline{(.)}$ is the average value of the corresponding random variable.

When an unsaturated device performs CCA, the probability that the channel is idle is P_i. Considering channel status for two consecutive slots using conditional probabilities yields $P_i = P_{i|i}P_i + P_{i|b}(1 - P_i)$, where $P_{i|i}$ ($P_{i|b}$) is the conditional probability that the channel is idle in the next slot given that channel state is idle (busy) in the current slot. By [18], [22], $P_{i|b} = 1/T_{tx}$. Then P_i can be rewritten as $P_i = 1/[1 + T_{tx}(1 - P_{i|i})]$.

Since sensing failure probability α can be considered the probability of a busy channel, we have $\alpha = 1 - P_i$. For unsaturated devices, R_{sv} is defined as the duration for serving a packet. A packet is called being served in the following two cases. The first case is the packet transmission. In this case, the duration includes the period of backoffs and the transmission duration. The other case is the packet drop due to K consecutive channel sensing failures. In this case, the duration only includes the period of K backoffs since no packet transmission occurs. Therefore, given the sensing failure probability α, the average duration to serve a packet $\overline{R_{sv}}$ for unsaturated devices is

$$\overline{R_{sv}} = \sum_{n=0}^{K-1} \alpha^n (1-\alpha) \left[\sum_{m=0}^{n} (b_m + 1) + T_{tx} \right] + \alpha^K \sum_{m=0}^{K-1} (b_m + 1),$$

where T_{tx} is the duration of a packet transmission, and b_m is the average interval in the mth backoff stage. The sensing attempt (i.e., CCA) probability τ for an unsaturated device with packets to transmit is

$$\tau = \sum_{n=0}^{K-1} \left[\frac{\alpha^n (1-\alpha)(n+1)}{\sum_{m=0}^{n} (b_m + 1) + T_{tx}} \right] + \frac{K\alpha^K}{\sum_{m=0}^{K-1} (b_m + 1)},$$

All of the above equations for unsaturated devices have their corresponding derivations for saturated devices. These derivations can be written simply by replacing $\overline{R_{sv}}$, α, τ, P_i, and $P_{i|i}$, with $\overline{R_{sv}^{'}}$, $\alpha^{'}$, $\tau^{'}$, $P_i^{'}$, and $P_{i|i}^{'}$, respectively.

The derivations of $P_{i|i}$ and $P_{i|i}^{'}$ are slightly different and described as follows. For an unsaturated device, it contends to access the channel only when packets are in the buffer waiting for transmission, which occurs with probability ρ. By [16], we have $\rho = \lambda \cdot \overline{R_{sv}}$, where λ is the packet arrival rate, and $\overline{R_{sv}}$ is the average packet service time. The conditional probability $P_{i|i}$ occurs only when no other device senses the channel in the current slot. For the unsaturated device, we have

$$P_{i|i} = (1-\tau')^{N^{'}} \sum_{n=0}^{N-N^{'}-1} \binom{N-N^{'}-1}{n} \rho^n (1-\tau)^n (1-\rho)^{N-N^{'}-n-1} \quad (1)$$

The part prior to the summation is the probability that no saturated device senses the channel. The remaining part denotes that among the $N - N^{'} - 1$ unsaturated devices, the total probability that n devices do not sense the channel with packets to transmit, while the other $N-N^{'}-n-1$ devices do not have packets to transmit, $0 \le n \le N - N^{'} - 1$. Similarly, $P_{i|i}^{'}$ can be derived as follows.

$$P_{i|i}' = (1-\tau')^{N^{'}-1} \sum_{n=0}^{N-N^{'}} \binom{N-N^{'}}{n} \rho^n (1-\tau)^n (1-\rho)^{N-N^{'}-n}. \quad (2)$$

From the balanced equations, the variables $\overline{R_{sv}}$, $\overline{R_{sv}^{'}}$, α, $\alpha^{'}$, τ, $\tau^{'}$, $P_{i|i}$, $P_{i|i}^{'}$, and ρ can be derived iteratively. With these variables known, the derivations of the fraction of sensing time, transmission time, and successful transmission time of the unsaturated and saturated devices are derived as follows.

Let T_{ca} be the interval for performing CCA. Then the fraction of sensing time η_{ca} of an unsaturated device is

$$\eta_{ca} = \rho \cdot \tau T_{ca},$$

and the fraction of sensing time $\eta_{ca}^{'}$ of a saturated device is

$$\eta_{ca}^{'} = \tau^{'} T_{ca}.$$

As we mentioned previously, when a packet is served in R_{sv}, the probability that the packet is transmitted is $(1-\alpha^K)$. Therefore, the fraction of transmission time of an unsaturated device is

$$\eta_{tx} = \rho(1-\alpha^K) T_{tx} / \overline{R_{sv}},$$

and the fraction of transmission time of a saturated device is

$$\eta_{tx}^{'} = (1-\alpha^K) T_{tx} / \overline{R_{sv}^{'}}.$$

Similarly, when a packet is transmitted, the successful probability is $P_{i|i}$. Therefore, the fraction of successful transmission time of an unsaturated device is

$$\eta_{sc} = \rho \cdot P_{i|i}(1-\alpha^K) T_{tx} / \overline{R_{sv}},$$

and the fraction of successful transmission time of a saturated device is

$$\eta_{sc}^{'} = P_{i|i}(1-\alpha^K) T_{tx} / \overline{R_{sv}^{'}}.$$

C. Modeling Buffered Packets

For low-power operation in IEEE 802.15.4, packets arriving from the upper layer during the inactive period are buffered. When measuring system performance, one must derive the distribution of buffered packets for devices. Let $P_k(t)$ be the probability that more than k packets arrive during the inactive period t, and packet inter-arrival time X follows a general cumulative distribution function F_X (i.e., $X \sim F_X$). Let $\hat{X}$ be the residual inter-arrival time of X with its corresponding distribution $F_{\hat{X}}(t)$, and X_i is the ith packet inter-arrival time in the inactive period. A packet residual inter-arrival time is defined as the duration from an intermediate moment between

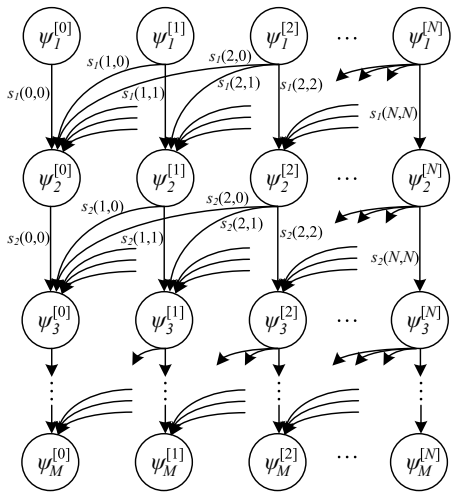

Fig. 3. The Markov chain model.

two consecutive packets to the arrival time of the immediate next packet [33]. Therefore, $\hat{X}$ in this model is the interval between the start time of the inactive period and the arrival time for the next packet. Then $P_k(t)$ can be derived as

$$\begin{aligned} P_k(t) &= P[\text{more than } k \text{ packets arrive in the inactive period } t] \\ &= P[\hat{X} + \textstyle\sum_{i=1}^{k-1} X_i \le t] \\ &= F_{\hat{X}}(t) \otimes F_X^{(k-1)}(t), \end{aligned}$$

where $\otimes$ represents the convolution operator, and $F_X^{(k-1)}(t)$ denotes the $(k-1)$-fold convolution of $F_X(t)$. Specifically, when F_X is an Exponential distribution, $P_k(t) = F_X^{(k)}(t) = 1 - G(k-1)$ due to the memory-less property, and G is the corresponding Poisson distribution with the same rate of F_X.

When F_X is a general distribution, the derivation of $P_k(t)$ is not straightforward. Since the derivational complexity of a multi-fold convolution is extremely high, the exact value is very difficult to derive accurately. To investigate the effects of various distributions F_X on system performance, an approximated $P_k(t)$ is adopted in the analysis. The detailed derivation process is as follows.

Define the random variable Y as $Y = \hat{X} + (k-1)X$ and F_Y is the cumulative distribution function of Y. Therefore, $P_k(t)$ equals to $F_Y(t)$. To derive the approximated $F_Y(t)$, the second-order Edgeworth approximation method [11] is utilized in this analysis. The detailed derivation is presented in Appendix A. According this derivation, the approximated $P_k(t)$ can be derived by a series of processes with n-th cumulants $E(X^n), n = 1, 2, \cdots, 5$, when the packet inter-arrival time X follows a general distribution. Since the second-order Edgeworth approximation method generates the approximated distribution based on a standard Normal distribution with a variance of 1, the distributions with an extremely large variance could be hard to capture by this approximation method. However, the traffic pattern in a sensor network is generally periodic, such that the traffic distribution with a large variance rarely occurs. Thus, this work adopts the second-order Edgeworth approximation method for analysis of a typical IEEE 802.15.4 network.

D. Derivation of System Performance Measures

In this subsection, the transmission of packets buffered during the inactive period in IEEE 802.15.4 are investigated using a non-stationary Markov Chain. Based on the beforehand analysis of Subsection IV-B and IV-C, queuing drop rate, goodput, and energy consumption can be derived.

For a device with buffer size M, queuing drops occur when more than M packets arrive during the inactive period $BI - SD$. Considering the entire BI, the queuing drop rate D can be obtained as follows.

$$D = \frac{1}{\lambda \cdot BI} \sum_{i=M+1}^{\infty} (i - M)[P_i(T) - P_{i+1}(T)].$$

Notably, $P_k(T)$ was derived in Subsection IV-C, where $T = BI - SD$.

Compared with the derivation of queuing drop rate, deriving goodput and energy consumption are more difficult since the behavior of buffered packet transmissions is considered. In a time region t_k, a state vector Ψ_k for the system is defined as

$$\Psi_k = \left\{ \psi_k^{[0]}, \psi_k^{[1]}, \cdots, \psi_k^{[N]} \right\},$$

where $\psi_k^{[n]}$ is the probability that n saturated devices exist in t_k. The transitions for the state vector, Ψ_k, is depicted with a non-stationary Markov Chain as shown in Figure 3, where $s_k(i,j)$ is the transition probability from $\psi_k^{[i]}$ to $\psi_{k+1}^{[j]}$. The time-varying transition matrix T_k can be expressed as

$$T_k = \begin{pmatrix} s_k(0,0) & 0 & 0 & \cdots & 0 \\ s_k(1,0) & s_k(1,1) & 0 & \cdots & 0 \\ s_k(2,0) & s_k(2,1) & s_k(2,2) & \cdots & \vdots \\ s_k(3,0) & s_k(3,1) & s_k(3,2) & \cdots & \vdots \\ \vdots & \vdots & \vdots & \ddots & \vdots \\ s_k(N,0) & s_k(N,1) & \cdots & \cdots & s_k(N,N) \end{pmatrix}.$$

Since a device is considered saturated in t_k, more than k packets arrive during the inactive period. Therefore, $s_k(i,j)$ follows a binomial distribution with the probability $P_k(T)$, where $T = BI - SD$.

$$s_k(i,j) = \binom{i}{j} [P_k(T)]^j [1 - P_k(T)]^{i-j}.$$

With the initial $\Psi_0 = \{0, 0, \cdots, 1\}$, the state vector for each t_k is given by

$$\Psi_{k+1} = \Psi_k T_k.$$

Here, the beforehand analysis derived in Subsection IV-B is utilized for the following derivations. Specifically, $(.)^{[n]}$ is the corresponding output with n saturated devices. Notably, average length of virtual time region t with n saturated devices is $\overline{R_{sv}^{'[n]}}$. Let $\overline{I}_b$ be the average interval for transmitting all packets buffered during the inactive period. Then we have

$$\overline{I}_b = \sum_{k=1}^{M} \sum_{n=0}^{N} \psi_k^{[n]} \overline{R_{sv}^{'[n]}}.$$

Let Υ_{sc} be the fraction of total successful transmission time in a BI for a device. For the active period SD in a

BI, the total successful transmission time includes successful transmission times in $\overline{I}_b$ and $(SD - T_{bn} - \overline{I}_b)$. Notably, $\overline{I}_b$ is the average interval for transmitting all buffered packets, and T_{bn} is the time for beacon reception.

This work first considers period $\overline{I}_b$. With the probability of $\psi_k^{[n]}$ that n saturated devices exist in t_k, $\eta_{sc}^{[n]}$ ($\eta_{sc}^{'[n]}$) is the fraction of successful transmission time of an unsaturated (saturated) device. Therefore, $\eta_{sc}^{[n]} \cdot R_{sv}^{[n]}$ and $\eta_{sc}^{'[n]} \cdot R_{sv}^{[n]}$ respectively denote the average successful transmission times for an unsaturated device and a saturated device in t_k. With N devices in the system, all combinations of n saturated devices and $N-n$ unsaturated devices are considered in each virtual time region. Since the maximum number of virtual time regions is M, average successful transmission time Ω_{sc} in $\overline{I}_b$ for a device is given as

$$\Omega_{sc} = \frac{1}{N} \sum_{k=1}^{M} \sum_{n=0}^{N} \psi_k^{[n]} \left[n \cdot \eta_{sc}^{'[n]} + (N-n) \eta_{sc}^{[n]} \right] \overline{R_{sv}^{'[n]}}. \quad (3)$$

Since all devices are unsaturated in the period $(SD - T_{bn} - \overline{I}_b)$, the average successful transmission time Ω'_{sc} for a device in this period is given as

$$\Omega'_{sc} = (SD - T_{bn} - \overline{I}_b) \eta_{sc}^{[0]}. \quad (4)$$

From equations (3) and (4), the fraction of total successful transmission time, Υ_{sc}, for a device is

$$\Upsilon_{sc} = \frac{\Omega_{sc} + \Omega'_{sc}}{BI}.$$

For throughput normalization, this work defines the goodput metric G as the fraction of achieved throughput to ideal throughput.

$$G = \frac{\Upsilon_{sc}}{\lambda \cdot T_{tx}}$$

The derivation of the fraction of total transmission time Υ_{tx} is similar to that for the fraction of total successful transmission time (Υ_{sc}); that is, η_{sc} in Υ_{sc} is replaced with η_{tx}. Thus we have

$$\Upsilon_{tx} = \frac{1}{BI} \left\{ \frac{1}{N} \sum_{k=1}^{M} \sum_{n=0}^{N} \psi_k^{[n]} \left[n \cdot \eta_{tx}^{'[n]} + (N-n) \eta_{tx}^{[n]} \right] \overline{R_{sv}^{'[n]}} + (SD - T_{bn} - \overline{I}_b) \eta_{tx}^{[0]} \right\}. \quad (5)$$

In a BI, total receiving time for a device includes the receiving time for CCA operation and beacon receiving time. The derivation for the fraction of total CCA time Υ_{ca} is similar to that of Υ_{tx}; that is, η_{tx} in Υ_{tx} is replaced with η_{ca}. Thus we have

$$\Upsilon_{ca} = \frac{1}{BI} \left\{ \frac{1}{N} \sum_{k=1}^{M} \sum_{n=0}^{N} \psi_k^{[n]} \left[n \cdot \eta_{ca}^{'[n]} + (N-n) \eta_{ca}^{[n]} \right] \overline{R_{sv}^{'[n]}} + (SD - T_{bn} - \overline{I}_b) \eta_{ca}^{[0]} \right\}. \quad (6)$$

From equation (6), the fraction of total receiving time, Υ_{rx}, for a device is

$$\Upsilon_{rx} = \frac{T_{bn}}{BI} + \Upsilon_{ca},$$

where T_{bn}/BI is the fraction of beacon receiving time.

For the inactive period, the fraction of total sleep time, Υ_{sp}, for a device is

$$\Upsilon_{sp} = 1 - \frac{SD}{BI}.$$

For a realistic analysis, this model also considers the time and energy expenditures resulting from hardware state transitions. The time spent in sleep-idle, idle-transmitting, and idle-receiving transition are T_{si}, T_{it}, and T_{ir}, respectively. Also, the energy consumed for sleep-idle, idle-transmitting, and idle-receiving transition are denoted as ϵ_{si}, ϵ_{it}, and ϵ_{ir}, respectively.

Since devices wake up at the start of each active period, the frequency of sleep-idle transition for a device Φ_{si} is $1/BI$. The frequency of idle-transmitting transition for a device Φ_{it} can be derived from Υ_{tx}. Thus, $\Phi_{it} = \Upsilon_{tx}/T_{tx}$.

The frequency of idle-receiving transition in a BI includes the frequencies for CCA operation and beacon reception. With the fraction of total CCA time Υ_{ca} derived in equation (6), the frequency of idle-receiving transition Φ_{ir} for a device is

$$\Phi_{ir} = \frac{1}{BI} + \frac{\Upsilon_{ca}}{T_{ca}},$$

where $1/BI$ is the frequency for beacon reception, and T_{ca} is the time spent for CCA operation.

Since the fraction of total idle time Υ_{id} for a device excludes the fractions of total transmission/receiving/sleeping times and all transition times, we have

$$\Upsilon_{id} = 1 - \sum_{s \in \{tx,rx,sp\}} \Upsilon_s - \sum_{s \in \{it,ir,si\}} T_s \Phi_s,$$

Finally, total energy consumption E in the system is

$$E = N \cdot \left(\sum_{s \in \{tx,rx,sp,id\}} E_s \Upsilon_s + \sum_{s \in \{it,ir,si\}} \epsilon_s \Phi_s \right),$$

where E_{tx}, E_{rx}, E_{sp}, and E_{id} are the energy expenditures per time unit for devices' states of transmitting, receiving, sleeping, and idle, respectively.

Conclusively, with system input parameters, queuing drop rate D, the goodput G, and the energy consumption E can be derived using the proposed analytical model.

V. Simulations and Numerical Results

In this section, the extensive network simulator NS-2 [31] is used for validation of the mathematical analysis and performance evaluation. In the simulation model, a star topology with 1 PAN coordinator and 10 devices is adopted. Each experimental result is obtained by averaging the results from 1,000 simulation runs, and each simulation run lasts 200,000 seconds. With the confidence level 95%, the confidence interval is within $\pm$ 1% of the sample mean of each data point. For a real-case study, this work adopts the power consumption model based on Chipcon CC2420EM/EB evaluation board and the $SmartRF^{TM}$ $Studio$ software [9], [7], [12], [22]. The energy parameters are set as follows. The energy expenditures for hardware transition are ϵ_{si}=691pJ, and ϵ_{it}=ϵ_{ir}=6.63μJ. The durations of hardware transitions are T_{si}=970μs, and T_{it}=T_{ir}=194μs. The energy expenditures per time unit for the four device states are $E_{tx} = 31.32mW$, $E_{rx} = 35.28mW$, $E_{sp} = 144nW$, and $E_{id} = 712\mu W$. Figure 4 shows the effects of buffer size on queuing drop rate, goodput, and energy

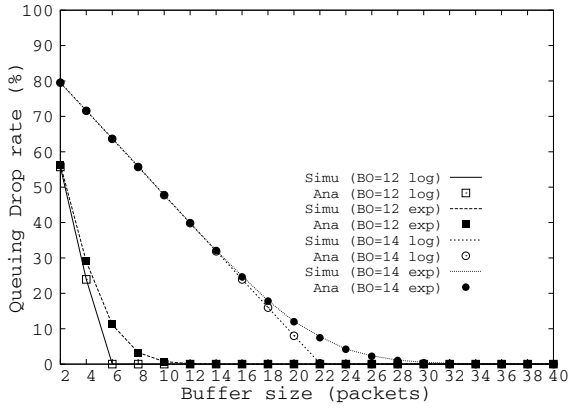

(a) Queuing drop rate

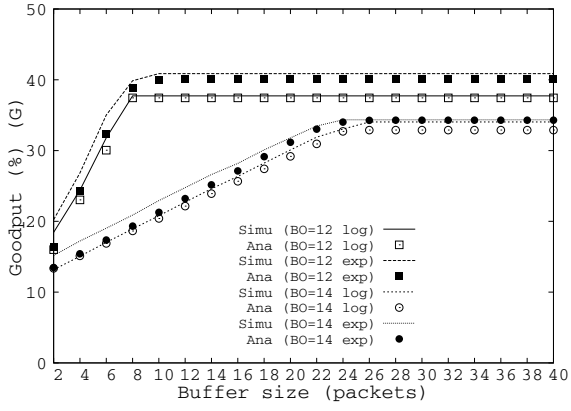

(b) Goodput

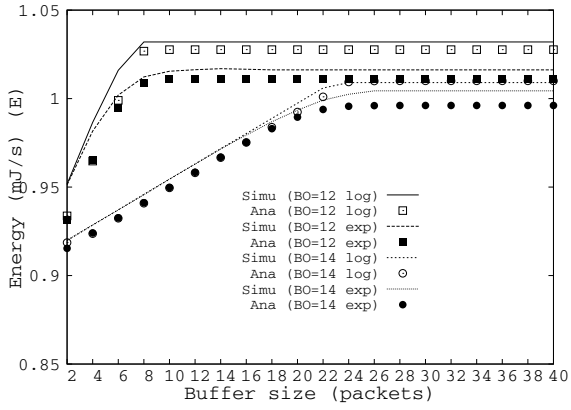

(c) Energy consumption

Fig. 4. The validation results.

consumption under different BOs (i.e. 12 and 14) with a duty cycle of 12.5%. In the experiment, traffic load is 0.1 packet per second, and packet inter-arrival times follow Exponential distribution with a variance of 100 and Lognormal distribution with a variance 0.01. The analytical results represented by dots match simulation curves closely, indicating that the analysis accurately captures the IEEE 802.15.4 low-power operation under the experimental settings.

For queuing drop rate, Figure 4 (a) shows that a large BO and small buffer size increase the drop rate due to an extended inactive period. Additionally, the traffic load distribution with a large variance (i.e. Exponential distribution) increases the drop rate, as the probability of buffer overflow is increased. For goodput and energy consumption in Figure 4 (b) and (c), large buffer size and smaller BO effectively increase goodput and thus increase energy consumption. Specifically, the traffic load distribution with a large variance increases goodput but decreases energy consumption.

Notably, the analytical model could not perform well when variance in the traffic load distribution was extremely large. The extensive experiment results indicate that the error rate could be as high as 60% when variance exceeds 1000. This phenomenon is caused by the limitation of the second-order Edgeworth approximation method in Section IV-C. However, the traffic pattern in a sensor network is typically periodic, such that a traffic distribution with a large variance rarely occurs.

To comprehensively investigate the effects of various traffic distributions on system performance, NS-2 based simulation experiments are conducted. Figure 5 and 6 show experimental results. This work uses a Gamma distribution with different shape parameters to simulate various distributions. The Gamma distribution is used because it can approximate many different traffic distributions and experimental data [15], [21]. The shape parameter ranges from 2^{-10} to 2^{10}. Notably, a small shape parameter increases variance. The traffic load is set to $1/s$, and system performance under three different BO values (i.e., $BO = 8, 11$, and 14) and two different buffer sizes (i.e., 10, and 10000) is evaluated with a duty cycle 50%. As depicted in Figure 4, system performance against the buffer size is affected most significantly when $M \leq 20$. When $M > 20$, queuing drop rate, goodput and energy consumption are typically stable. Therefore, we adopt $M = 10$ and $M = 10000$ to respectively represent the two cases of $M \leq 20$ and $M > 20$ for further performance analysis.

In an IEEE 802.15.4 network, system throughput degradation is mainly caused by three packet loss: queuing drop, failure drop, and collision drop. Queuing drop occurs when a packet arrives in a full buffer. Failure drop and collision drop uniquely exist in the contention based MAC protocols. Specifically, the failure drop occurs when a retransmission attempt reaches a predefined limitation. In the IEEE 802.15.4 CSMA/CA mechanism, the device can retransmit a packet up to three times. Additionally, collision drop occurs when two devices transmit packets simultaneously over a wireless channel.

Figure 5 presents evaluation results for the three packet drops. Figure 5 (a) shows the results of queuing drop rate. Since queuing drops rarely occur in a large buffer, the curves of M=10000 approximate 0. Conversely, high drop rate is caused under a small shaper parameter when M=10 because traffic load with a large variance increases queuing drops. Figure 5(b) shows the results of the failure drop rate. All curves increase as the shape parameter increases. It is because a small variance in traffic distribution decreases the diversity of buffered packet number and thus the channel contention becomes more serious. For the curves of M=10000, a large BO increases the failure drop rate since the increased buffer packets burdens the channel contention. Conversely, the curves of M=10 indicate that a large BO causes a small failure drop rate, since the dominant high queuing drop rate markedly decreases the packets for channel contention. Notably, the

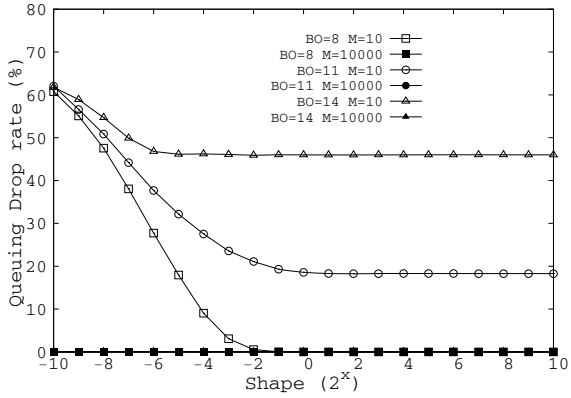

(a) Queuing drop rate

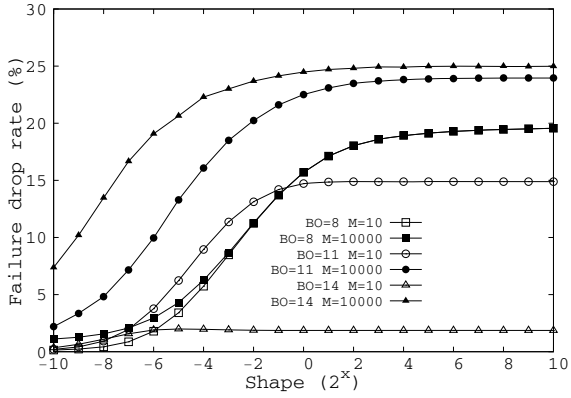

(b) Failure drop rate

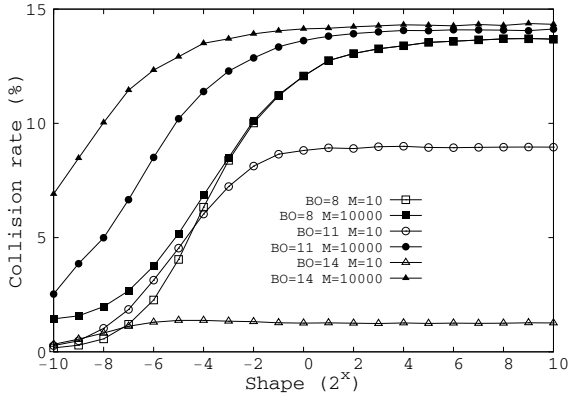

(c) Collision rate

Fig. 5. The packet loss.

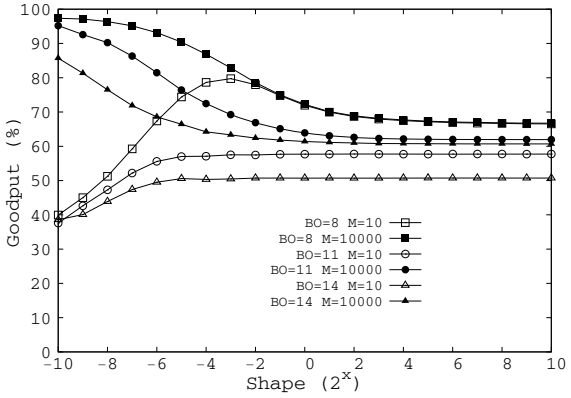

(a) Goodput

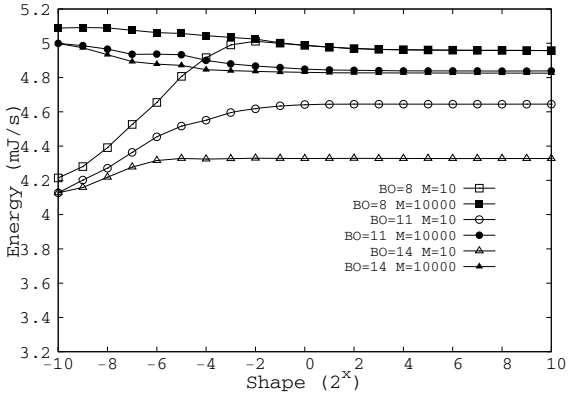

(b) Energy consumption

Fig. 6. The goodput and energy consumption.

curve of $BO = 11$ is unexpectedly higher than that of $BO = 8$ especially when the shape is less than 2^{-1}. Since the failure drop rate of $BO = 11$ is much higher than that of $BO = 8$ without a buffer limitation (see the curves of M=10000), the failure drop rate has greater effects on system performance than the queuing drop rate. Figure 5(c) shows the results of the collision drop rate. The curves in this figure are similar to that in Figure 5 (b). Specifically, the collision drop rates for all curves of M=10000 are extremely high when the shape is large, indicating that collision drop has a higher sensitivity for traffic congestion than other packet drops.

In Figure 6, goodput and energy consumption are evaluated under the same system settings. In Figure 6 (a), the goodput is implicitly the compound effect of the three packet drop rates in Figure 5. Generally, the curves of M=10 increase as the shape increases, since the decreasing queuing drop dominates goodput degradation. On the other hand, the curves of M=10000 decrease as the shape increases, because the goodput degradation is only caused by failure drop and collision drop. Specifically, the curve of M=10 with $BO = 8$ increases and then decreases as the shape increases. This is because queuing drop has little impact (approaches 0) when the shape exceeds 2^{-2} and the failure drop and collision drop dominate goodput.

Figure 6 (b) presents the results of the energy consumption. The curves for energy consumption are similar to those for goodput since most the energy is consumed by packet sending (including the carrier sensing and actual transmission) in this experimental setup. However, some substantial differences are observed and described below. Since the channel contention is serious when the shape is large (see Figure 5 (b)(c)), additional energy is consumed by the additional carrier sensing and retransmissions. Therefore, the curves of energy consumption have a larger scale than those of goodput. Additionally, three curves of different BO values with M=10000 are close because the absence of a queuing drop makes the carrier sensing and retransmissions dominate energy consumption, such that the beacon overhead effects are comparably less significant.

Conclusively, when buffer size is sufficient, the traffic load distribution with a small variance contributes to considerable

channel contention, such that goodput is degraded and energy consumption is increased. Conversely, goodput and energy consumption are dominated by queuing drop when buffer size is limited. Therefore, determining a best set of system parameter inputs for low-power operation of an IEEE 802.15.4 network is not straightforward.

VI. Conclusion

The IEEE 802.15.4 MAC layer provides a duty-cycle operation by setting two system parameters, BO and SO, to achieve low power consumption for ZigBee devices. This work presented a comprehensive analysis of IEEE 802.15.4 duty-cycle operation. Specifically, an novel analytical model that accommodates a general traffic distribution was developed. An NS-2 based simulation model validated by the developed analytical model was also proposed. Through the experiments conducted by the analytical and simulation models, it was shown that our analysis properly captures the behavior of IEEE 802.15.4 low-power operation. Furthermore, some important performance-evaluation insights were given, and can be guidelines for future low-power Zigbee network deployment.

For future research, the models will be extended to accommodate contention free periods for analysis of IEEE 802.15.4 low-power operation.

VII. Acknowledgement

This work was supported in part by the Excellent Research Projects of National Taiwan University under Contract 98R0062-05, by the National Science Council under Contract NSC95-2118-M-009-004-MY2, NSC95-2221-E-002-096-MY3, and NSC96-2219-E-002-004, and by the Institute of Information Industry.

Appendix

A. The Approximation for $P_k(t)$ Using the Second-order Edgeworth Approximation

For a random variable Z with zero mean and unit variance, the second-order Edgeworth approximation of the probability density function (pdf) and cumulative density function (cdf) of Z, denoted as f_Z and F_Z, respectively, is written as

$$f_Z(z) = \theta(z)\left[1 + \frac{\delta_3 H_3(z)}{6} + \frac{\delta_4 H_4(z)}{24} + \frac{\delta_3^2 H_6(z)}{72}\right]$$

$$F_Z(z) = \Theta(z) - \theta(z)\left[\frac{\delta_3 H_2(z)}{6} + \frac{\delta_4 H_3(z)}{24} + \frac{\delta_3^2 H_5(z)}{72}\right],$$

where θ and Θ stand for the pdf and cdf of the standard normal distribution, respectively. Note that the approximation is especially suitable for the random variables with the Normal distribution properties. H_2, H_3, H_4, H_5, and H_6 are the Hermite polynomials defined as $H_2(z) = z^2 - 1, H_3(z) = z^3 - 3z, H_4(z) = z^4 - 6z^3 + 3, H_5(z) = z^5 - 10z^3 + 15z, H_6(z) = z^6 - 15z^4 + 45z^2 - 15$, respecitvely. Also, $\delta_3 = E(Z^3)$ and $\delta_4 = E(Z^4) - 3$ stand for the 3rd and 4th order cumulants of Z, respectively.

To apply the second-order Edgeworth approximation method for the derivation of $F_Y(t)$, Z is defined as $Z = (Y - \mu_Y)/\sigma_Y$ to have zero mean and unit variance, where μ_Y is the mean of Y and σ_Y is the standard deviation of Y. Therefore, $F_Y(t)$ can be written as $F_Z[(t - \mu_Y)/\sigma_Y]$.

The derivations of $F_Z[(t - \mu_Y)/\sigma_Y]$ are described as follows. First, we have $\mu_Y = E(Y)$ and $\sigma_Y = \sqrt{E(Y^2) - (E(Y))^2}$. For the derivations of δ_3 and δ_4 in the approximation, $E(Y^3)$ and $E(Y^4)$ are required. To avoid redundancy, only the derivation of $E(Y)$ is described here. The derivations of $E(Y^2)$, $E(Y^3)$ and $E(Y^4)$ can be done in a similar approach, and the details are omitted.

$$E(Y) \quad = E(\hat{X} + (k-1)X) = E(\hat{X}) + (k-1)E(X).$$

In the above equation, $E(X)$ can be directly derived from F_X, and $E(\hat{X})$ can be derived by utilizing the excess life theorem [23]. Then we have

$$E(\hat{X}) = \frac{E(X^2)}{2 \cdot \mu_X}.$$

where μ_X is the mean of X.

Finally, the approximated $P_k(t)$ can be derived by a series of process with n-th cumulants $E(X^n), n = 1, 2, \cdots, 5$, when the packet inter-arrival time X follows a general distribution.

References

[1] 802.15.3-2003 IEEE Standard for Information Technology-Part 15.3: wireless medium access control (MAC) and physical layer (PHY) specifications for wireless personal area networks (WPANs), 2003.

[2] 802.15.4-2003 IEEE Standard for Information Technology-Part 15.4: wireless medium access control (MAC) and physical layer (PHY) specifications for low-rate wireless personal area networks (LR-WPANs), 2003.

[3] G. Anastasi, M. Conti, E. Gregori, and A. Passarella, "Saving energy in Wi-Fi hotspots through 802.11 PSM: an analytical model," in *Workshop on Modeling and Optimization in Mobile, Ad Hoc and Wireless Networks (WiOpt)*, Mar. 2004.

[4] D. Bertsekas and R. Gallager, *Data Networks*, 2nd ed. Prentice Hall, 1992.

[5] G. Bianchi, "Performance analysis of the IEEE 802.11 distributed coordination function," *IEEE J. Select. Areas Commun.*, vol. 18, no. 3, pp. 535-547, Mar. 2000.

[6] M. Bottigliengo, C. Casetti, C.-F. Chiasserini, and M. Meo, "Short-term fairness for TCP flows in 802.11b WLANs," in *Proc. IEEE INFOCOM*, Mar. 2004.

[7] B. Bougard, F. Catthoor, D. C. Daly, A. Chandrakasan, and W. Dehaene, "Energy efficiency of the IEEE 802.15.4 standard in dense wireless microsensor networks: modeling and improvement perspectives," in *Proc. Design Automation and Test in Europe Conference and Exhibition (DATE)*, Mar. 2005.

[8] L. X. Cai, X. Shen, J. W. Mark, and Y. Xiao, "Voice capacity analysis of WLAN with unbalanced traffic," *IEEE Trans. Veh. Technol.*, vol. 55, pp. 752-761, May 2006.

[9] Chipcon. 2004. 2.4 GHz IEEE 802.15.4/Zigbee-ready RF transceiver, http://www.chipcon.com/.

[10] P. Djukic and S. Valaee, "Reliable and energy efficient transport layer for sensor networks," in *Proc. IEEE Globe Communications Conference (Globecom)*, Nov. 2006.

[11] F. Y. Edgeworth, "The law of error," *Trans. Cambridge Philosophical Society*, 1905.

[12] S. Pollin *et al.*, "Performance analysis of slotted carrier sense IEEE 802.15.4 medium access layer," *IEEE Trans. Wireless Commun.*, vol. 7, no. 9, Sept. 2008.

[13] J. A. Gutierrez, "On the use of IEEE 802.15.4 to enable wireless sensor networks in building automation," in *Proc. IEEE International Symposium on Personal, Indoor and Mobile Radio Communications (PIMRC)*, Sept. 2004.

[14] J. Jeon, J. W. Lee, J. Y. Ha, and W. H. Kwon, "DCA: Duty-Cycle Adaptation Algorithm for IEEE 802.15.4 beacon-enabled networks," in *Proc. IEEE Vehicular Technology Conference (VTC)*, Spring 2007.

[15] N. L. Johnson and S. Kotz, *Continuous Univariate Distributions-1*. New York: John Wiley & Sons, 1970.

[16] L. Kleinrock, *Queueing Systems*. John Wiley & Sons, 1975.

[17] J.-S. Lee, "Performance evaluation of IEEE 802.15.4 for low-rate wireless personal area networks," *IEEE Trans. Consumer Electron.*, vol. 52, no. 3, pp. 742-749, Aug. 2006.
[18] X. Ling, Y. Cheng, J. W. Mark, and X. Shen, "Analysis of contention access part of IEEE 802.15.4 MAC," *IEEE Trans. Wireless Commun.*, vol. 7, no. 6, pp. 2340-2349, June 2008.
[19] J. Mišić, S. Shaf, and V. B. Mišić, "Performance of a beacon enabled IEEE 802.15.4 cluster with downlink and uplink traffic," *IEEE Trans. Parallel and Distributed Syst.*, vol. 17, pp. 361-376, Apr. 2006.
[20] M. Neugebauer, J. Plonnigs, and K. Kabitzsch, "A new beacon order adaptation algorithm for IEEE 802.15.4 networks," in *Proc. European Workshop on Wireless Sensor Networks (EWSN)*, Jan. 2005.
[21] X. Ning and C. G. Cassandras, "Dynamic sleep time control in event-driven wireless sensor networks," in *Proc. IEEE Conference on Decision and Control (CDC)*, Dec. 2006.
[22] I. Ramachandran, A. Das, and S. Roy, "Analysis of contention access part of IEEE 802.15.4 MAC," *ACM Trans. Sensor Networks*, vol. 14, Aug. 2007.
[23] S. M. Ross, *Introduction to Probability Models*. New York: Academic, 1985.
[24] S.-T. Sheu, Y.-Y. Shih, and L.-W Chen, "An adaptive interleaving access scheme (IAS) for IEEE 802.15.4 WPANs," in *Proc. IEEE Vehicular Technology Conference (VTC)*, Spring 2005.
[25] F. Shu, T. Sakurai, H. L. Vu, and M. Zukerman, "Optimizing the IEEE 802.15.4 MAC," in *Proc. IEEE Region 10 Conference (TENCON)*, Nov. 2006.
[26] F. Shu, T. Sakurai, M. Zukerman, and H. L. Vu, "Packet loss analysis of the IEEE 802.15.4 MAC without acknowledgements," *IEEE Commun. Lett.*, vol. 11, pp. 79-81, Jan. 2007.
[27] P. Si, H. Ji, F. R. Yu, and G. Yue, "IEEE 802.11 DCF PSM Model and a novel downlink access scheme," in *Proc. IEEE Wireless Communications and Networking Conference (WCNC)*, Apr. 2008.
[28] Bluetooth SIG, Bluetooth Specification, 1999.
[29] M.-Y. Chung, T.-J. Lee, and H.-R. Lee, "MAC throughput limit analysis of slotted CSMA/CA in IEEE 802.15.4 WPAN," *IEEE Commun. Lett.*, vol. 10, pp. 561-563, July 2006.
[30] Z. Tao, S. Panwar, D. Gu, and J. Zhang, "Performance analysis and a proposed improvement for the IEEE 802.15.4 contention access period," in *Proc. IEEE Wireless Communications and Networking Conference (WCNC)*, 2006.
[31] The NS-2 Simulator, http://www.isi.edu/nsnam/ns/.
[32] Y.-C. Tseng, C.-S. Hsu, and T.-Y. Hsieh, "Power-saving protocols for IEEE 802.11-based multi-hop ad hoc networks," in *Proc. IEEE INFOCOM*, June 2002.
[33] Y. Zhang, "Performance modeling of energy management mechanism in IEEE 802.16e mobile WiMAX," in *Proc. IEEE Wireless Communications and Networking Conference (WCNC)*, Mar. 2007.
[34] Zigbee Alliance, http://www.zigbee.org.

Yu-Kai Huang received his B.S. degree in Department of Computer Science from National Tsing Hua University, Taiwan, in 2003, and M.S. degree in Department of Computer Science and Information Engineering from National Taiwan University, Taiwan, in 2005. He is currently working toward the Ph.D. degree in Graduate Institute of Networking and Multimedia, National Taiwan University, Taiwan. His current research interests are focused on low-rate wireless personal area networks, especially in resource management and energy efficient issues.

Ai-Chun Pang received the B.S., M.S. and Ph.D. degrees in Computer Science and Information Engineering from National Chiao Tung University, Taiwan, in 1996, 1998 and 2002, respectively. She joined the Department of Computer Science and Information Engineering (CSIE), National Taiwan University (NTU), Taipei, Taiwan, in 2002. Currently, she is an Associate Professor in CSIE and Graduate Institute of Networking and Multimedia of NTU, Taipei, Taiwan. Her research interests include design and analysis of personal communications services network, mobile computing, voice over IP and performance modeling.

Hui-Nien Hung received the Ph.D. degree in statistics from The University of Chicago, Chicago, IL, in 1996. He is currently a Professor in the Institute of Statistics, National Chiao Tung University, Hsinchu, Taiwan. His research interests include applied probability, biostatistics, statistical inference, statistical computing, and industrial statistics.